Design of a high-power near-infrared collimation optical system

CHANG CHENG SUN[1], YUN CUI ZHANG[1,*], YAN WANG[1], AI LIN CHEN[1], ZHE XU[1], YANQIU ZOU[2], JIYU XU[2], SHUAI WANG[2]
[1]*School of Information Science & Engineering, Dalian Polytechnic University, Dalian, China*
[2]*Dalian Estar Intelligent Technology Co., Ltd., Dalian 116600, China*

With the development of infrared lighting technology, it is necessary to design infrared lighting systems for different lighting purposes. This paper presents a design method for the high-power infrared optical system. In this design, the system is composed of the high-power infrared laser diode light source array and the freeform surface lens array. The light source has a power of 125 W and a divergent angle of 10°×25°. The collimation system is designed for the light source, which reaches an energy utilization of 95% and a divergent angle of 0.5°. The system can be adapted to remote night-vision monitoring sites.

(Received May 11, 2023; accepted October 9, 2023)

Keywords: High-power, Small divergent angle, High irradiance, Remote lighting

1. Introduction

With the growing demand for high-power, specialized spectral light sources, laser diode (LD) light sources have garnered increasing attention. The emission of light is achieved through electrical stimulation of a doped semiconductor material, such as InGaN. Consequently, the material emits photons with specific energy levels and thus within a narrow range of wavelengths. Recently, an automotive industrial lighting system utilizing LD as the light source has been introduced [1-3].

The LD has been developed rapidly due to unique light output characteristics including a directional beam pattern and a small light-emitting area. They can be used as light sources for the lighting system exhibiting huge potential for applications in vehicle headlights, night detective equipment, as well as indoor long-distance lighting [4-8]. The emitted spectrum encompasses special wavelengths like visible light, infrared, and ultraviolet; particularly near-infrared plays a crucial role in night vision lighting.

Infrared compensation systems are pivotal in fields such as photography and nighttime monitoring [9-15]. For night vision lighting purposes, the far transmission distance of near-infrared light significantly enhances illumination range during low-light conditions. A common technique involves concentrating energy into collimated light that can be irradiated over longer distances using optical lenses. These lenses are designed to redistribute intensity by emitting beams parallel to the main optical axis. An original reflectionless meta-surface gradient-refractive-index collimating meta-lens composed of amorphous silicon posts convert wide-angle radiation into small-angle radiation with a half divergent angle of 7° and 63% transmission efficiency; this lens holds promise for future advanced imaging applications [16]. The meta-surface lenses composed of amorphous silicon posts on a flat sapphire substrate efficiently collimate the output beam that has a half divergent angle of 0.36° and 79% transmission efficiency, which is applied in chemical sensing for environmental and medical monitoring [17]. Moreover, several works have shown that the divergent angle and transmission efficiency can be further narrowed by the combination of multiple optical lenses. The ternary lens group based on the principle of focal free magnification consists of a fixed lens group, variable multiplier lens group, and compensating lens group, the collimation is freely adjusted by the variable multiplier lens group to produce the appropriate size of the spot, which is used in the field of light distance measurement [18]. Compared with traditional optical lenses, the light can be precisely controlled by the freeform surface lens. The beam of the light source is redistributed into two collimated beams with different wavelengths and different angles, which is used in the near-infrared spectrometer [19].

Micro-lens arrays play a crucial role in various optical systems, offering enhanced optical functionalities and

improved performance. By employing microlens array technology to design collimating lenses for infrared laser light sources, the optical system can achieve highly precise control and manipulation of the light field by arranging numerous tiny lenses in a specific geometric structure. This significantly expands the functionality and application range of the optical system. The miniaturization and manufacturability advantages of microlens arrays bring about higher optical performance and smaller size requirements for digital micro-lens devices using multi-step lithography technology in the field of optics, meeting the continuous demands of modern scientific and technological development for optical devices [20-22]. Based on individual design and random arrangement of micro-lenses, a random microlens array composed of different random micro-lenses is designed to achieve efficient and uniform beam shaping [23]. Multi-step lithography based on digital micromirror devices proposes a flexible and efficient strategy for manufacturing user-defined microstructure arrays. Micro-lens arrays with custom distribution of square and hexagonal shapes are fabricated using multi-step lithography, enabling rapid fabrication of 2D lattice structures with periodic/aperiodic spatial distribution and arbitrary shapes [24]. Maskless lithography technology based on digital micromirror devices allows quick production of hexagonal compound eye microlens array by layer-by-layer lithographing the hexahedral array while adapting to variable curvature profiles to improve reconstruction accuracy [25].

In this paper, we primarily research the collimated lens design method of infrared LD light source. This design aims to promote irradiance and energy utilization and narrow the divergent angle, which can be used for long-distance night detection areas. The divergent angle of the infrared LD light source is collimated through the freeform surface lens, and the power is greatly improved by the array design of LD and freeform surface lens to increase the brightness of the remote operation area.

2. The design of the optical system

In this design, the optical system is designed for high-power near-infrared spectroscopy LD light sources The design of the freeform surface lens for LD light source is significantly researched, which can redistribute the light to irradiate the further distance.

2.1. The selection of LD

The parameters of the infrared system are mainly affected by the performance of the LD, which has a single wavelength. The light source is 905 nm single wavelength produced by Osram, the power reaches 125 W, and the irradiance reaches 12500 W/m². The light source structure parameters are shown in Fig. 1.

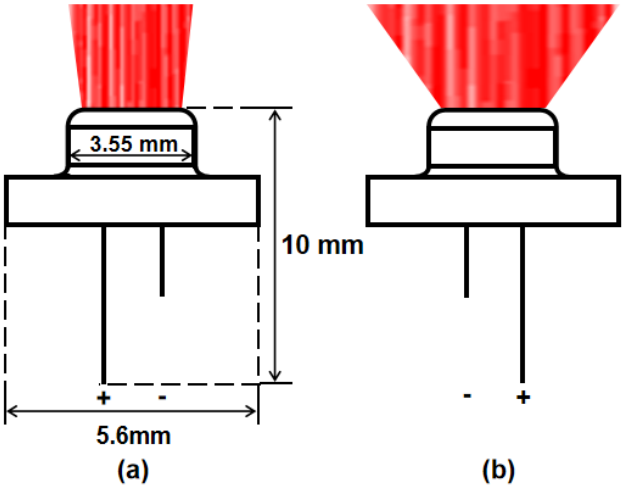

Fig. 1. The light source structure parameters

Fig. 1 shows the profile structure of the LD on the x-axis and y-axis. Fig. 1(a) shows the profile structure on the x-axis, the size of the optical structure is 5.6 mm × 10 mm, and the aperture of the circular luminous surface is 3.55 mm. Fig. 1(b) shows the profile structure on the y-axis. To ensure higher collimation, LD with single wavelength and unidirectional luminescence is selected. The optical parameters of the light source are shown in Fig. 2.

Fig. 2 shows the three-dimensional structure of the LD divergent angle. Fig. 2(a) shows the asymmetric divergent angle of the LD, the divergent angle of the x-axis is θ_x and the y-axis is θ_y. Fig. 2(b) shows the light distribution curve of the x-axis and y-axis. With the increase of real-time current $I_{current}$, the maximum divergent angle of the x-axis is 10° and the y-axis is 25°.

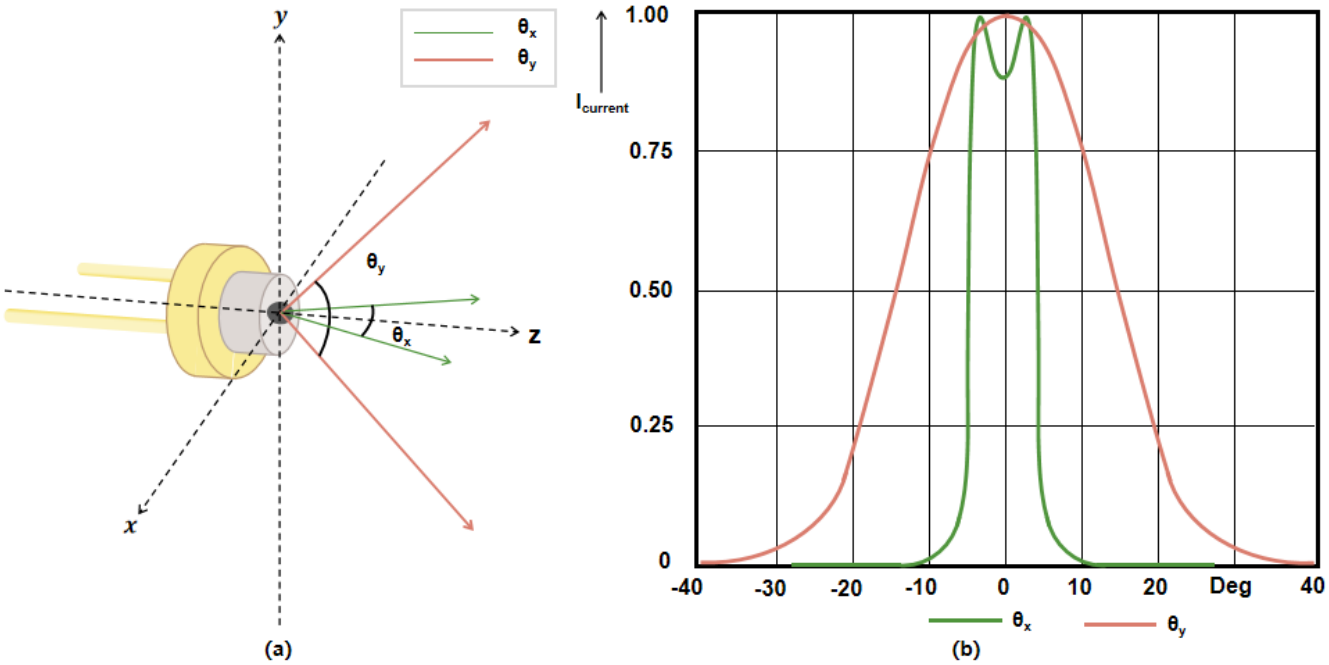

Fig. 2. The optical parameters of the light source (color online)

2.2. The design of the freeform surface lens

The divergent angle of the LD light source is collimated through the freeform surface lens. The refractive index of lens material has a significant influence on the transmittance of the LD light source. The material of the freeform surface lens is PMMA with the refractive index of 1.49, and the transmittance reaches 95%. The divergent angle of the LD light source is asymmetric, and the divergent angle of the x-axis and y-axis are collimated respectively. The structure of the freeform surface lens designed based on the freeform surface design method is shown in Fig. 3.

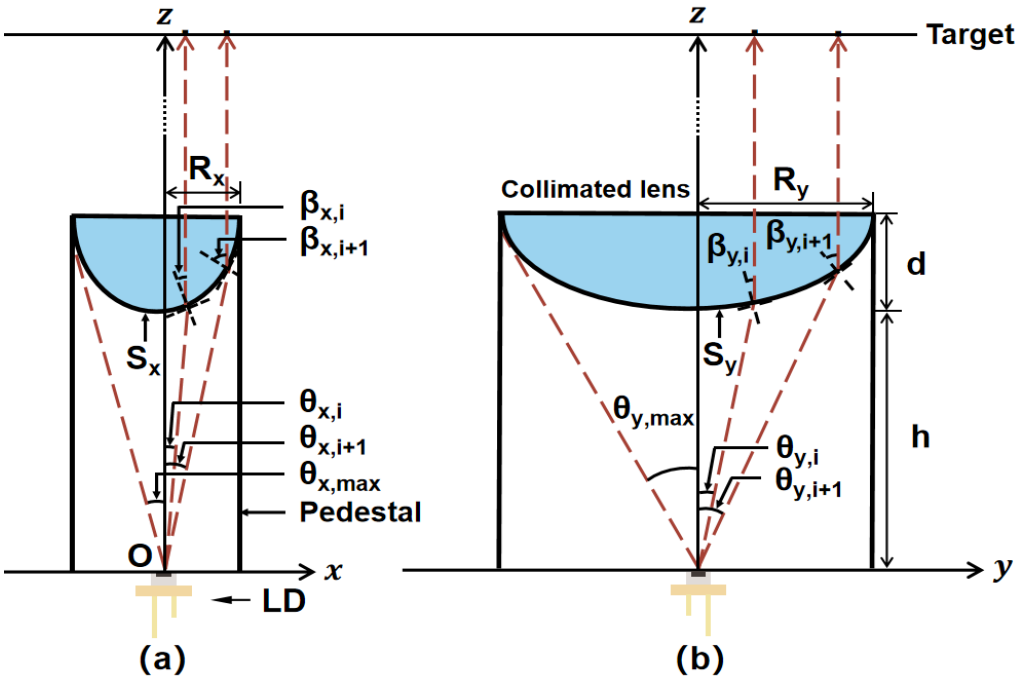

Fig. 3. The freeform surface lens structures (color online)

Fig. 3 shows the profile structure of the light emitted parallel to the main optical axis through the freeform surface lens. Fig. 3(a) shows the profile structure of the freeform surface lens on the x-axis, the divergent angle from 0° to 8° of the light is refracted and collimated out through the freeform surface S_x parallel to the x-axis. According to Snell's law, Equation (1) is shown the free curve of the freeform surface S_x parallel to the x-axis

$$n_0 \bullet sin(\theta_{x,i} + \beta_{x,i}) = n_1 \bullet sin\,\beta_{x,i} \quad (1)$$

where n_0 is the refractive index of air, n_1 is the refractive index of the freeform surface lens, $\theta_{x,i}$ is the divergent angle of the LD light source on the x-axis, $\beta_{x,i}$ is the refraction angle of the freeform surface lens on the x-axis

Fig. 3(b) shows the profile structure of the freeform surface lens on the y-axis, the divergent angle from 0° to 25° of the light is refracted and collimated out through the freeform surface S_y parallel to the y-axis. According to Snell's law, Equation (2) is shown the free curve of the freeform surface S_y parallel to the y-axis

$$n_0 \bullet sin(\theta_{y,i} + \beta_{y,i}) = n_1 \bullet sin\,\beta_{y,i} \quad (2)$$

where $\theta_{y,i}$ is the divergent angle of the LD light source on the y-axis, $\beta_{y,i}$ is the refraction angle of the freeform surface lens on the y-axis

The slope of each point on the free curve parallel to the x-axis and y-axis is obtained by collating Equation (1) and Equation (2), which are shown in Equation (3) and Equation (4)

$$k_{x,i} = \frac{n_0 \bullet sin\,\theta_{x,i}}{n_1 - n_0 \bullet cos\,\theta_{x,i}} \quad (3)$$

$$k_{y,i} = \frac{n_0 \bullet sin\,\theta_{y,i}}{n_1 - n_0 \bullet cos\,\theta_{y,i}} \quad (4)$$

where $k_{x,i}$ is the slope of the free curve S_x, and $k_{y,i}$ is the slope of the free curve S_y.

The coordinates of each point on the free curve parallel to the x-axis can be obtained by substituting Equation (3) into the coordinate iteration Equation (5) and Equation (6)

$$x_{x,i+1} = \frac{(y_{x,i} - k_{x,i} \bullet x_{x,i}) \bullet tan\,\theta_{x,i+1}}{1 - k_{x,i} \bullet tan\,\theta_{x,i+1}} \quad (5)$$

$$y_{x,i+1} = \frac{y_{x,i} - k_{x,i} \bullet x_{x,i}}{1 - k_{x,i} \bullet tan\,\theta_{x,i+1}} \quad (6)$$

where $\theta_{x,i}$ corresponds to the point E_i $(x_{x,i}, y_{x,i})$ on the free curve parallel to the x-axis, $\theta_{x,i+1}$ corresponds to the point E_{i+1} $(x_{x,i+1}, y_{x,i+1})$ on the free curve. Several discrete points calculated by Equation (5) and Equation (6) are connected to form the contour of the free curve parallel to the x-axis. The freeform surface S_x is formed by rotating about the x-axis.

The coordinates of each point on the free curve parallel to the y-axis can be obtained by substituting Equation (4) into the coordinate iteration Equation (7) and Equation (8)

$$x_{y,i+1} = \frac{(y_{y,i} - k_{y,i} \bullet x_{y,i}) \bullet tan\,\theta_{y,i+1}}{1 - k_{y,i} \bullet tan\,\theta_{y,i+1}} \quad (7)$$

$$y_{y,i+1} = \frac{y_{y,i} - k_{y,i} \bullet x_{y,i}}{1 - k_{y,i} \bullet tan\,\theta_{y,i+1}} \quad (8)$$

where $\theta_{y,i}$ corresponds to the point e_i $(x_{y,i}, y_{y,i})$ on the free curve parallel to the y-axis, $\theta_{y,i+1}$ corresponds to the point e_{i+1} $(x_{y,i+1}, y_{y,i+1})$ on the free curve. Several discrete points calculated by Equation (7) and Equation (8) are connected to form the contour of the free curve parallel to the y-axis. The freeform surface S_y is formed by rotating about the z-axis

The width and length of the supplementary lighting range are mainly affected by the freeform surface lens. The width and length of the freeform surface lens are determined by the divergent angle of the LD light source on the x-axis and y-axis. The relationship between the semi-aperture of the freeform surface lens and the divergent angle on the x-axis and y-axis are shown in Equation (9) and Equation (10)

$$R_x = h \times \tan\theta_{x,max} \quad (9)$$

$$R_y = h \times \tan\theta_{y,max} \quad (10)$$

where R_x and R_y are the x-axis and y-axis semi-aperture of freeform surface lens, h is the working distance of the LD lens, $\theta_{x,max}$ is the 8° maximum divergent angle of the LD light source on the x-axis, $\theta_{y,max}$ is the 25° maximum divergent angle of the LD light source on the y-axis.

The collimation and brightness can be freely adjusted by changing the distance between the LD and the freeform surface lens. The high distance ratio of the freeform surface lens is shown in Equation (11)

$$\delta = \frac{h}{\mathrm{d}} \tag{11}$$

where, δ is the high distance ratio of the freeform surface lens, and d is the thickness of the freeform surface lens.

3. Experiment and simulation

The LD is coordinated with the freeform surface lens that has been designed and analyzed in an optical channel of the infrared system. As a supplement to the night vision performance of the illumination system, the infrared system has 8 LD light sources. The total power reaches 1000 W, and the divergent angle is 0.5°. The installation is positioned around the illumination system to improve the ability to accurate tracking at long distances.

3.1. The physical production process

The lighting requirements usually need to consider the atmospheric attenuation at sea level, and an optical channel cannot meet the requirements of supplementary lighting. The infrared system is composed of an optical channel array design, which can greatly improve the power to produce sufficient brightness. The simulation structure model of the collimation system is shown in Fig. 4.

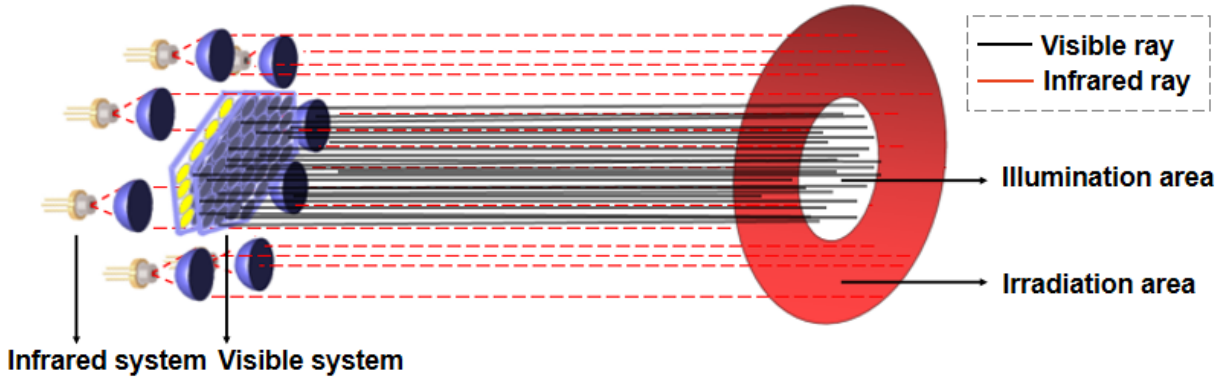

Fig. 4. The simulation structure of the collimation system (color online)

Fig. 4 shows the optical structure of the visible system and the infrared system, the light emitted from the visible system produces a visible light illumination area, and the light emitted from the infrared system is collimated to form an irradiation area. The infrared system differs in terms of method, function, and application. In terms of design method, the infrared system focuses light to create an illumination area. Functionally, the infrared system employs an array design within their optical channels that significantly enhances their ability to generate sufficient brightness. In practical application, infrared lighting systems find frequent use in areas such as infrared night vision equipment, security monitoring, and other specialized fields. It should be noted that stable operational efficiency and ample brightness are ensured by the infrared LD light source, which allows it to adapt to various low-light working environments within infrared systems.

3.2. The simulation results of an optical channel

The optical parameters of the infrared system depend on an optical channel that has the optical properties of high brightness, high collimation, and small divergent angle. The simulation results of the LD light source are shown in Fig. 5.

Fig. 5 shows the simulation results of an LD light source. Fig. 5(a) shows that the light diverges to the target plane at a distance of 200 m. Fig. 5(b) shows the simulation effect of light emitted from the LD light source in the x-axis and y-axis directions. Fig. 5(c) shows that the irradiance effect is a narrow strip, the irradiance range reaches 35 m × 93 m, the energy unevenly distributes in the target plane, and the maximum irradiance is 0.38 W/m². Fig. 5(d) shows that the irradiance distribution in the x-axis and y-axis directions is asymmetrical. The divergent angle of the LD is shown in Fig. 6.

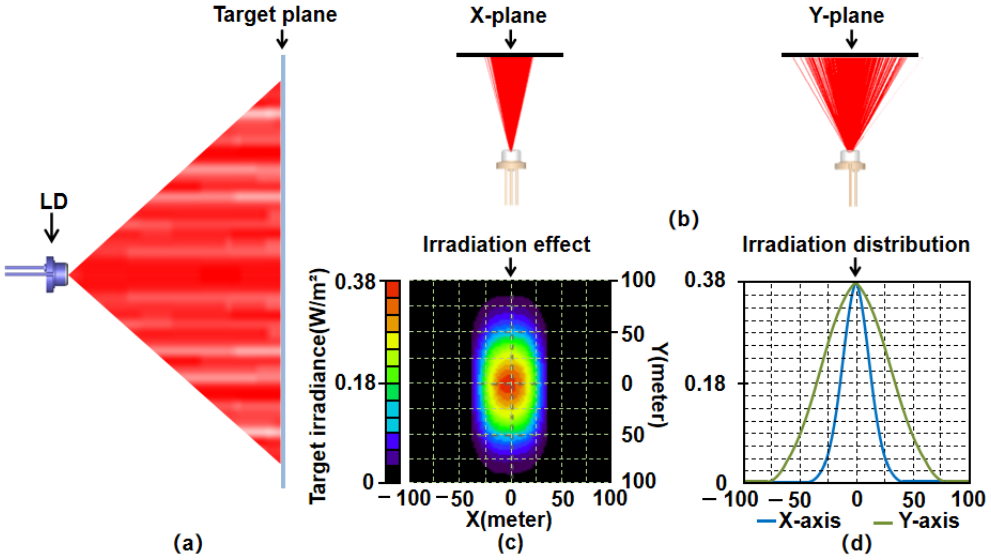

Fig. 5. The simulation results of the LD light source (color online)

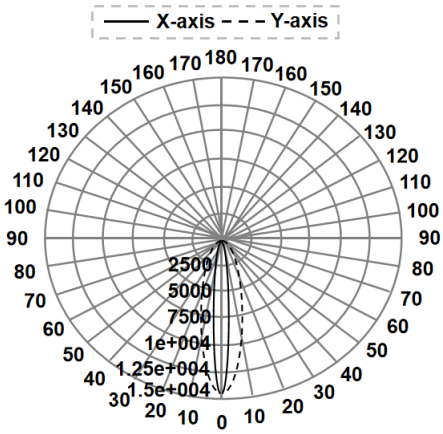

Fig. 6. The divergent angle of LD

Fig. 6 shows that the divergent angle of the LD light source is 10° × 25° on the x-axis and y-axis directions. The LD light source without a light distribution design cannot be used for remote lighting. In terms of evaluating the performance of this new design, the simulation results of an optical channel are shown in Fig. 7.

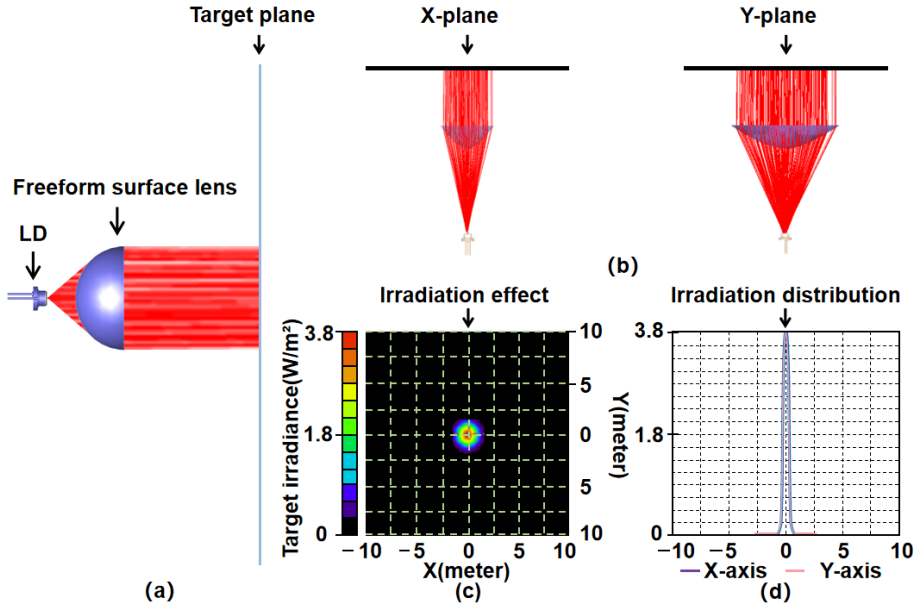

Fig. 7. The simulation results of an optical channel (color online)

Fig. 7 shows the simulation results of an optical channel. Fig. 7(a) shows that the light is collimated out to the target plane of a distance of 200 m through the freeform surface lens. Fig. 7(b) shows the simulation effect of an optical channel in the x-axis and y-axis directions. Fig. 7(c) shows that the irradiance effect of an optical channel is greatly narrowed compared with the irradiance effect of an LD light source, the irradiance range is limited to the 1.7 m, the energy is concentrated in a circle, and the maximum irradiance reaches 3.8 W/m². Fig. 7(d) shows that the irradiance distribution in the x-axis and y-axis directions is greatly narrowed through the freeform surface lens. The divergent angle of an optical channel is shown in Fig. 8.

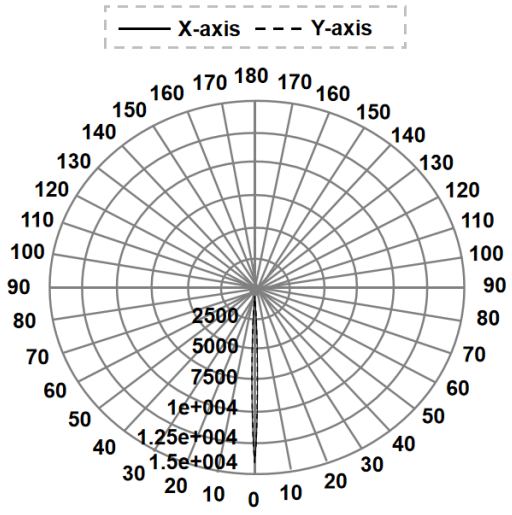

Fig. 8. The divergent angle of an optical channel

Fig. 8 shows that the divergent angle of an optical channel reaches 0.5°, and the light is emitted parallel to the main optical axis to meet the lighting requirements at a long distance.

4. Performance analysis of the collimation system

This paper has presented a theoretical and experimental study of the collimation process of the LD light source, the infrared system consists of 8 LD light sources with freeform surface lenses. According to the lowest lighting usage requirements at 200 m, the minimum irradiance is 100 W/m², the maximum divergent angle is 2°, and the minimum energy utilization is 0.65. In order to verify the rationality of the lowest lighting requirements mentioned above, we change the high distance ratio and semi-aperture of the freeform surface lens. In the process of changing the parameters of the freeform surface lens, if the values generated by the parameters meet the requirements, the numerical values are proven to be feasible.

4.1. Irradiance analysis

In infrared transmission, the radiation brightness reached within a certain distance is an important parameter that determines the performance of the system. The focal length between the freeform surface lens and LD lighting source has been controlled by the high distance ratio, while the number of rays emitted from the lens have been influenced by the semi-aperture. However, it is important to note that there are practical constraints on varying these parameters due to factors such as manufacturing capabilities, optical system requirements, and target application. In our study, a range of high-distance ratios and x-axis semi-apertures within specified design conditions have been explored. The effect of the high distance ratio and the x-axis semi-aperture of the freeform surface lens on the irradiance is shown in Fig. 9.

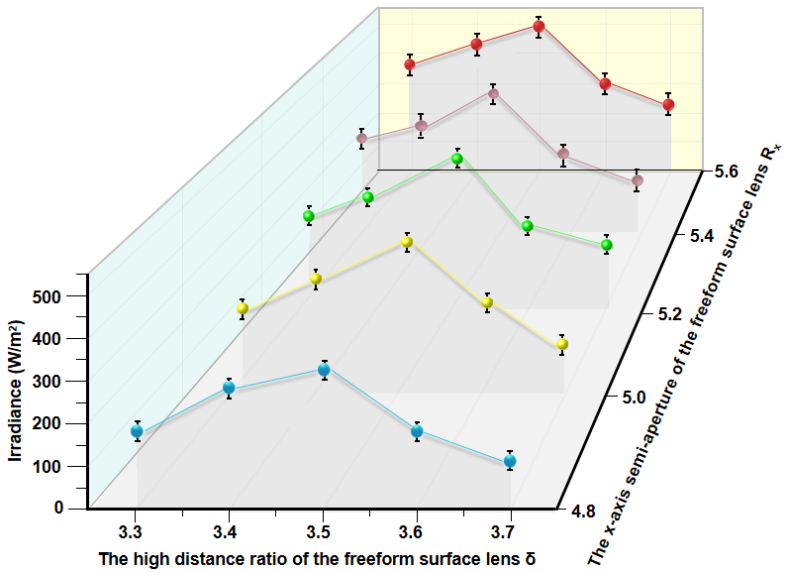

Fig. 9. The effect of the high distance ratio and the x-axis semi-aperture of the freeform surface lens on the irradiance (color online)

Fig. 9 illustrates how different x-axis semi-apertures R_x ranging from 4.8 mm to 5.6 mm affect irradiance about the high distance ratio δ. By analyzing this relationship, the optimal parameter combination that meets the requirements of irradiance and divergence angle has been determined: a maximum irradiance of 500 W/m² was achieved with a high distance ratio of 3.5 and an x-axis semi-aperture of 5.6 mm. These results demonstrate that our selected parameter range effectively meets irradiation requirements under challenging design conditions. In addition, during the design process for infrared lighting optical systems, considerations must be given to overall length and caliber limitations imposed by size restrictions on components such as infrared laser sources and collimating lenses due to diffraction and scattering effects experienced by infrared light during transmission processes. Therefore, careful optical design is necessary to ensure system performance.

4.2. Divergent angle analysis

The divergent angle of the infrared system light should be minimized to ensure efficient transmission over longer distances. A crucial interaction exists between irradiance and the divergent angle, which can distinctly show that the high distance ratio acts as a limiting factor for the divergent angle. Therefore, it is essential to design both the high distance ratio and x-axis semi-aperture within a range consistent with conditions used for irradiance analysis. This design approach ensures that the range of divergence angles satisfies minimum illumination requirements at 200 m. The effect of the high distance ratio and the x-axis semi-aperture of the freeform surface lens on the divergent angle is shown in Fig. 10.

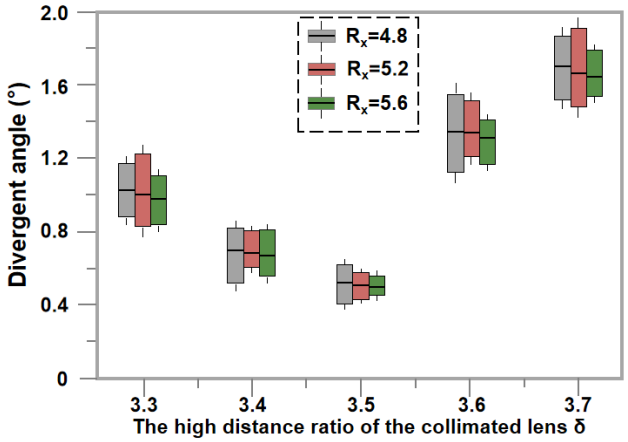

Fig. 10. The effect of the high distance ratio and the x-axis semi-aperture of the freeform surface lens on the divergent angle (color online)

Fig. 10 demonstrates that for the freeform surface lens, the divergent angle reaches its minimum value at a high distance ratio of 3.5. With further consideration during the design process, it is possible to reduce this divergence angle to 0.5° when utilizing an x-axis semi-aperture of 5.6 for the freeform surface lens. Our data demonstrated that there is a certain effect on collimation and divergence angles in optical systems due to varying distances between infrared laser sources and infrared collimating lenses. Specifically, increasing the distance between the infrared laser source and the infrared collimated lens can effectively reduce the divergent angle and improve the beam formation, and a larger aperture can provide more incident light and enhance the lighting effect.

4.3. Energy utilization analysis

The transmission distance of irradiation is mainly affected by energy utilization. To verify the feasibility of the new method, we also carry out the simulation adopting energy utilization as an evaluation index of light performance. Differing from divergent angle analysis, if the divergent angle was small, the energy utilization would become large due to the more energy concentrated in the light. The effect of the high distance ratio and the x-axis semi-aperture of the freeform surface lens on energy utilization is shown in Fig. 11.

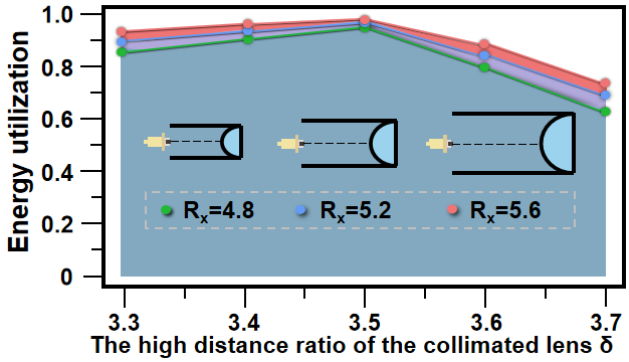

Fig. 11. The effect of the high distance ratio and the x-axis semi-aperture of the freeform surface lens on energy utilization (color online)

As shown in Fig. 11, the energy utilization reaches the maximum of 0.95 when the high distance ratio of the freeform surface lens is 3.5 and the x-axis semi-aperture of the freeform surface lens is 5.6. This trend of change suggests that energy utilization is mainly affected by the distance between the LD light source and the freeform surface lens. The results of these data indicate that the high distance ratio was the dominant factor affecting energy utilization.

5. Conclusion

In this paper, we present a collimation approach based on the freeform surface lenses for the infrared LD light source. The simulation results demonstrate that the lens achieves a collimating beam with an irradiance of 500 W/m², divergent angle of 0.5°, and energy efficiency of 95% under the high distance ratio of 3.5 and the semi-aperture of 5.6 mm. Small beam angle and high energy utilization are important factors to ensure the application of the system in high-power night vision scenarios. The optical system designed by this method can be used as a laser diode light source in many fields.

Acknowledgments

First, I would like to thank my tutor, Professor Yuncui Zhang. From topic selection, collection, and writing to the final draft, this paper was all completed under the careful guidance of my tutor. Her careful and rigorous working attitude has greatly influenced and helped me, which has benefited me for a lifetime. Reflecting on the tireless and patient instruction Zhang gave me, I shall always remember these valuable experiences and spiritual treasures. I would like to express my heartfelt thanks to the esteemed Zhang. Second, I would like to express my sincere thanks to Yan Wang for his guidance and help during the design process. Third, thanks are due to Ailin Chen and Zhe Xu for their assistance with the experiments and to Yanqiu Zou, Jiyu Xu, and Shuai Wang for valuable discussions.

References

[1] BMW Group, “BMW Laserlicht geht in Serie. Der BMW i8 ist das erste Serienfahrzeug mitder innovativen Lichttechnologie” (2014), accessed on 2015-01-05.
[2] AUDI AG, “Weltpremiere auf der CES 2014 in Las Vegas: Der Audi Sport quattro laserlight concept” (2014), accessed on 2015-01-05.
[3] K. Pudenz, “Mercedes-Benz Concept GLA bekommt Scheinwerfer mit Laserlicht” (2014), accessed on 2015-01-05.
[4] Łukasz Zinkiewicz, Jakub Haberko, Piotr Wasylczyk, Opt. Express **23**, 4206 (2015).
[5] Zehua Liu, Shuxing Li, Yihua Huang, Lujie Wang, Yirong Yao, Tao Long, Xiumin Yao, Xuejian Liu, Zhengren Huang, Ceramics International **44**, 16 (2018).
[6] Jiuru He, Rui Song, Weiqiang Yang, Jing Hou, Opt. Express **29**, 19140 (2021).
[7] Yang Ou, Bin Zhang, Ke Yin, Zhongjie Xu, Shengping Chen, Jing Hou, Opt. Express **26**, 9822 (2018).
[8] Zhenlv Lv, Juan Liu, Jiasheng Xiao, Ying Kuang, Opt. Express **26**, 32802 (2018).
[9] Meng Xu, Xinyue Wang, Jiexin Weng, Jingling Shen, Yanbing Hou, Bo Zhang, Opt. Express **30**, 40611 (2022).
[10] Jiang Xin-Yang, Liu Wei-Wei, Li Tian-Xin, Xia Hui, Deng Wei-Jie, Yu Li, Li Yu-Ying, Lu Wei, Opt. Express **31**, 7090 (2023).
[11] I. Sakon, T. Onaka, T. Ootsubo, H. Matsuhara, J. Noble, M. C. Clampin, G. G. Fazio, H. A. Macewen, J. M. Oschmann, Proc. SPIE **8442**, 44 (2012).
[12] H. S. Lee, V. R. Shrestha, S. S. Lee, Optics Communications **291**, 242 (2013).
[13] Shuang Lin, Dan Zhang, Yuanfei Jiang, Anmin Chen, Mingxing Jin, Opt. Express **30**, 17026 (2022).
[14] Shao-Yung Lee, Chih-Hsien Cheng, Kun-You Huang, Xin Chen, Kangmei Li, Chia-Hsuan Wang, Ming-Jun Li, Chao-Hsin Wu, Gong-Ru Lin, Opt. Express **30**, 17130 (2022).
[15] Tong Hoang Tuan, Shunei Kuroyanagi, Kenshiro Nagasaka, Takenobu Suzuki, Yasutake Ohishi, Opt. Express **26**, 16054 (2018).
[16] Chenyu Wu, Zhe Liu, Zhiguo Yu, Xinlin Peng, Zehua Liu, Xuejian Liu, Xiumin Yao, Yun Zhang, Opt. Express **28**, 19085 (2020).
[17] Yanze Gao, Zhuo Li, Sichen Zhang, Tianze Zhao, Rui Shi, Qingfeng Shi, Opt. Express **29**, 41428 (2021).
[18] Chih-Ting Yeh, Yen-I Chou, Kai-Shing Yang, Shih-Kuo Wu, Chi-Chuan Wang, Opt. Express **27**, 7226 (2019).
[19] Chiara Lindner, Jachin Kunz, Simon J. Herr, Sebastian Wolf, Jens Kießling, Frank Kühnemann, Opt. Express **29**, 4035 (2021).
[20] D. H. Dinh, H. L. Chien, Y. C. Lee, Optics & Laser Technology **113**, 407 (2019).
[21] Yv'ang Chen, Yuncui Zhang, Minjv Fan, Da Pan, Shuhan Yan, Journal of Modern Optics **69**(12), 684 (2022).
[22] S. L. Aristizabal, G. A. Cirino, A. N. Montagnoli, A. A. Sobrinho, J. B. Rubert, M. Hospital, R. D. Mansano, Optical Engineering **52**(12), 125101 (2012).
[23] Zhongyuan Liu, Hua Liu, Zifeng Lu, Qiankun Li, Jinhuan Li, Optics Communications **443**, 211 (2019).
[24] Ying Zhang, Jun Luo, Zheng Xiong, Hua Liu, Li Wang, YingYing Gu, ZiFeng Lu, Jin Huan, JiPeng Huang, Opt. Express **27**(22), 31956 (2019).
[25] B. Yang, J. Zhou, Q. Chen, L. Lei, K. Wen, Opt. Express **26**(22), 28927 (2018).

*Corresponding author: zhang_yc@dlpu.edu.cn